IVYSPRING INTERNATIONAL PUBLISHER

Theranostics

2017; 7(7): 1928-1939. doi: 10.7150/thno.18719

Research Paper

^{177}Lu-Labeled Phosphoramidate-Based PSMA Inhibitors: The Effect of an Albumin Binder on Biodistribution and Therapeutic Efficacy in Prostate Tumor-Bearing Mice

Cindy J. Choy[1]*, Xiaoxi Ling[2]*, Jonathan J. Geruntho[2], Sophia K. Beyer[1], Joseph D. Latoche[2], Beatrice Langton-Webster[1], Carolyn J. Anderson[2, 3, 4, 5]✉ and Clifford E. Berkman[1]✉

1. Cancer Targeted Technology, Woodinville, WA;
2. Department of Medicine, University of Pittsburgh, Pittsburgh, PA 15203;
3. Department of Radiology, University of Pittsburgh, Pittsburgh, PA 15203;
4. Department of Bioengineering, University of Pittsburgh, Pittsburgh, PA 15203;
5. Department of Pharmacology & Chemical Biology, University of Pittsburgh, Pittsburgh, PA 15203.

* Co-first authors

✉ Corresponding authors: Clifford E. Berkman, Ph.D., Cancer Targeted Technology, Woodinville, WA 98072 Tel: 509-335-7613 Fax: 509-335-8389 Email: cberkman@cancertargetedtechnology.com Carolyn J. Anderson, PhD., Department of Medicine, University of Pittsburgh, Pittsburgh, PA 15203 Phone: 412-624-6887 Fax: 412-624-2598 Email: andersoncj@upmc.edu

Received: 2016.12.12; Accepted: 2017.03.06; Published: 2017.04.27

Abstract

Prostate-specific membrane antigen (PSMA) continues to be an active biomarker for small-molecule PSMA-targeted imaging and therapeutic agents for prostate cancer and various non-prostatic tumors that are characterized by PSMA expression on their neovasculature. One of the challenges for small-molecule PSMA inhibitors with respect to delivering therapeutic payloads is their rapid renal clearance. In order to overcome this pharmacokinetic challenge, we outfitted a ^{177}Lu-labeled phosphoramidate-based PSMA inhibitor (CTT1298) with an albumin-binding motif (CTT1403) and compared its *in vivo* performance with that of an analogous compound lacking the albumin-binding motif (CTT1401). The radiolabeling of CTT1401 and CTT1403 was achieved using click chemistry to connect ^{177}Lu-DOTA-N_3 to the dibenzocyclooctyne (DBCO)-bearing CTT1298 inhibitor cores. A direct comparison *in vitro* and *in vivo* performance was made for CTT1401 and CTT1403; the specificity and efficacy by means of cellular uptake and internalization, biodistribution, and therapeutic efficacy were determined for both compounds. While both compounds displayed excellent uptake and rapid internalization in PSMA+ PC3-PIP cells, the albumin binding moiety in CTT1403 conferred clear advantages to the PSMA-inhibitor scaffold including increased circulating half-life and prostate tumor uptake that continued to increase up to 168 h post-injection. This increased tumor uptake translated into superior therapeutic efficacy of CTT1403 in PSMA+ PC3-PIP human xenograft tumors.

Key words: PSMA, albumin, phosphoramidate, ^{177}Lu, radiotherapy.

Introduction

Early efforts to target the enzyme-biomarker Prostate-specific membrane antigen (PSMA) were aimed at the development of PSMA-targeted imaging [1-16] and therapeutic agents [17-20] for prostate cancer. This was initially attributed to its high degree of expression on prostate cancer cells, especially for late-stage, androgen-independent, and metastatic prostate tumors [21-23]. However, the endothelial expression of PSMA on neovasculature of various non-prostatic tumors such as kidney, bladder, lung, breast, colorectal, pancreatic cancers, and melanoma [9, 24, 25] has raised the prospect of its use in these diseases.

Various chemical scaffolds have been developed as inhibitors of PSMA's enzymatic activity, some of which have been pursued as PSMA targeting

molecules for imaging and therapeutic agents. It is well recognized that a significant advance in prostate cancer therapy could be achieved if the simplicity and affinity of these small-molecule PSMA inhibitors could be harnessed in an effective platform to deliver chemo- and/or radio-therapeutic payloads. Indeed, promising therapeutic efficacy results have emerged recently for two urea-based PSMA inhibitors (PSMA Imaging and Therapy (I&T) and the commercially available PSMA-617) bearing 1,4,7,10-tetraazacyclododecane-1,4,7,10-tetraacetic acid (DOTA) analogs and complexed with Lu-177 ($T_{1/2}$ = 6.7 d; 100% β- emission) [26-30]. The advantage of employing DOTA analogs in these compounds is that they can also be complexed with Ga-68, thus transforming these molecules into PSMA-targeted positron emission tomography (PET) imaging agents.

One of the challenges for small-molecule PSMA inhibitors with respect to delivering therapeutic payloads is their rapid renal clearance. This is due to their highly charged nature (poly-carboxylate), but this charge is also necessary for their high affinity to PSMA. In order to overcome this pharmacokinetic challenge [31], we outfitted a ^{177}Lu-labeled PSMA inhibitor with an albumin-binding motif [32] and compared its *in vivo* performance with that of an analogous compound without this motif (**Scheme 1**). This albumin-binding motif has been shown to reduce receptor-mediated kidney uptake and increase tumor uptake of a ^{177}Lu-labeled folate analog [33]. For the remaining design elements of these compounds, CTT1298 was selected as the PSMA-targeting molecule due to its high-affinity and irreversible binding to PSMA, and its extensive internalization by PSMA-expressing tumor cells [14, 15]. As described previously for this class of PSMA inhibitors [16], radiolabeling using click chemistry was selected in order to protect the targeting molecule from the conditions needed for radiolabeling the DOTA chelator. Elevated temperatures under extended acidic conditions lead to hydrolysis of phosphoramidate P-N bond. Installing ^{177}Lu into the DOTA chelator separately spared the targeting molecule from the relatively harsh radiolabeling conditions. The click-ready dibenzocyclooctyne (DBCO)-derivatized CTT1298 platforms (CTT1400, which has no albumin binding motif, and CTT1402, which does bind albumin) are versatile in that therapeutic and diagnostic cargo can be conveniently substituted. Here we present the synthesis of two novel PSMA inhibitors (CTT1400 and CTT1402) and preparation of the ^{177}Lu-labeled agents (CTT1401 and CTT1403) through click chemistry with ^{177}Lu-DOTA-azide. Cell uptake and internalization, biodistribution and the initial therapeutic efficacy studies in mouse models of these two ^{177}Lu-labeled PSMA-targeted inhibitors are described herein, with the goal to choose the best agent to optimize the dose and determine dosimetry and toxicity.

Materials and Methods

Experiments on laboratory mice were performed in accordance with and approved by the University of Pittsburgh Institutional Animal Care and Use Committee (IACUC). Male, athymic nude mice (NCr nude, 6-8 weeks) were purchased from Charles River Laboratories (Wilmington, MA). Mice were housed in groups of 3-4 in ventilated cages on hardwood chip bedding in the same room. Food and water were provided *ad libitum*. Mice were acclimated for at least 72 h prior to any procedures.

Synthesis of Radiolabeling Precursors CTT1400 and CTT1402

The preparation of the radiolabeling precursors CTT1400 and CTT1402 are fully detailed in the Supplemental Material.

Radiolabeling

Synthesis of ^{177}Lu-DOTA-azide: To a 0.5 M NH_4OAc buffer (0.16 mL, pH = 4.95) was added DOTA-azide (10 µL, 53 nmol), gentisic acid (10 µL, 0.56 µmol) and $^{177}LuCl_3$ (up to 10 µL, 0.54 GBq). The resulting mixture was heated at 95 °C for 1 h. For quality control, a small aliquot (2.0 µL) of the mixture was diluted with 0.5 M NH_4OAc buffer (20 µL, pH = 4.95) before injection for high-pressure liquid chromatography (HPLC) analysis (see Supplemental Material, **Table S6**). High radiolabeling yield (>95%), high radiolabeling purity (>95%) and specific activity (up to 28 MBq/nmol) were observed. The mixture was used in the next step without further purification. The ^{177}Lu-labeled PSMA-targeted constructs are referred to as CTT1401 (derived from CTT1400) and CTT1403 (derived from CTT1402).

Synthesis of CTT1401

A solution of CTT1400 (17 µL, 0.34 µmol) was added to the freshly prepared ^{177}Lu-DOTA-azide mixture. The resulting mixture was heated at 37 °C for 1 h before HPLC separation (**Table S7**). CTT1401 fractions were collected in 200 µL portions. Fractions with the highest radioactivity were consolidated and concentrated using nitrogen gas flow at 41 °C. The final solution was diluted with saline for injection. For quality control, a small aliquot was analyzed by HPLC. High conversion of ^{177}Lu-DOTA-azide (>95%), high radiolabeling yield (>95%), and high radiolabeling purity (>95%) were observed.

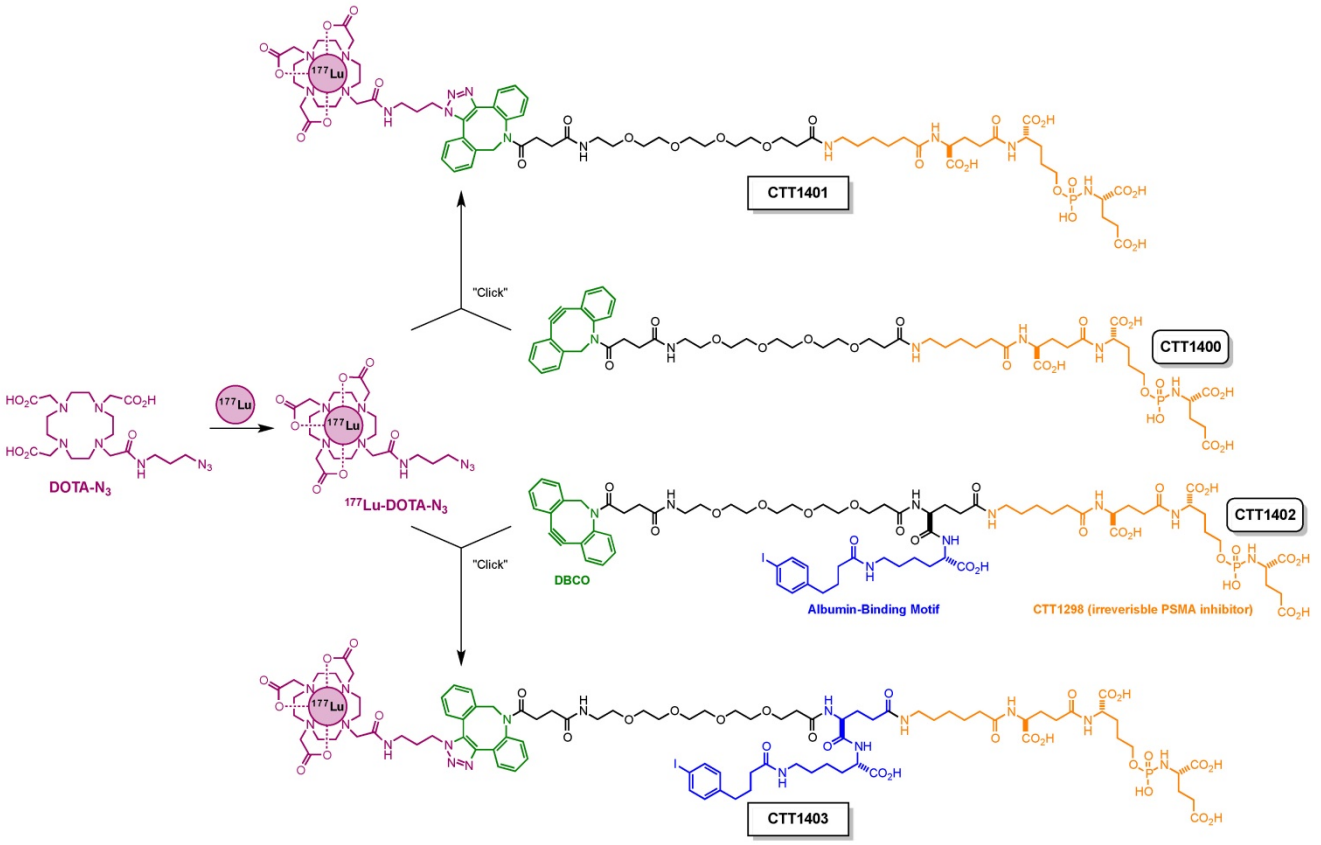

Scheme 1. Modular assembly of CTT1401 and CTT1403.

Synthesis of CTT1403

CTT1403 was prepared similarly to CTT1401 using CTT1402 and ^{177}Lu-DOTA-azide mixture. After reaction, the separation and quality control was achieved using HPLC (see Supplemental Material, **Table S8**). A high conversion rate of ^{177}Lu-DOTA-azide (>95%), high radiolabeling yield (>95%), and high radiolabeling purity (>95%) was observed. Specific activities ranged from 1-28 MBq/nmol.

In Vitro Studies

The human prostate cancer cell lines PC3-WT (PSMA negative) and PC3-PIP (PSMA positive) were obtained through the American Type Culture Collection and from Dr. Martin Pomper (John Hopkins University), respectively. Cells were propagated in standard growth media (RPMI-1640 supplemented with 10% Fetal Bovine Serum (FBS), 100 units/mL Penicillin, and 100 µg/mL Streptomycin) in a humidified incubator at 37 °C under 5% CO_2. Each cell line was passaged to around 70% confluence, with isolation performed using trypsin (0.25%, 0.1% EDTA) for 12-18 min.

Cells were plated separately (4.0 x 10^5 cells/well) in 12 well plates and incubated overnight, using 1 mL of standard growth media per well. All cells were washed with internalization buffer (50 mM HEPES, 100 mM NaCl, 1% FBS) and incubated for 30 min with either 47 µg (208 nmol) 2-(phosphonomethyl)pentane-1,5-dioic acid (2-PMPA) in internalization buffer (blocking) or standard internalization buffer. Wells were washed, followed by the addition of CTT1401 or CTT1403 (30 kBq, 1.1 pmol), and incubated for 15, 30, 60, 120, or 240 min at 37 ˚C. To collect surface bound fractions at each time point, samples were washed with internalization buffer followed by 10 min incubation with 20 mM sodium acetate in Hank's Balanced Salt Solution (HBSS, pH 4.0). The solution was removed and saved, followed by a wash of 20 mM sodium acetate in HBSS without incubation, and the pooling of the two solutions. The cells were then lysed by rinsing each well with 0.5% sodium dodecyl sulfate (SDS) in double distilled water ($_{dd}H_2O$) x2. All samples were counted using a Cobra II automated gamma-counter. To determine percent initial dose per milligram, protein concentration was measured in duplicate with a Pierce BCA Protein Assay Kit (Thermo Fisher, Waltham, MA) using Bovine Serum Albumin (BSA) as a standard on the Synergy H4 Hybrid Reader (BioTek, Winooski, VT).

Stability Studies in Mouse Serum

Mouse blood was collected via cardiac puncture of the left ventricle with a 25G needle. Blood was placed into heparin-coated microfuge tubes (Sarstedt Inc, Nümbrecht, DE) and allowed to sit at room temperature for 1 hour. Tubes were then centrifuged at 5000 rpm for 5 min to separate serum for stability studies. CTT1403 (9.3 MBq; 0.10 mL) was incubated with 0.50 mL mouse serum for 1, 4, 24 h at 37 °C. At each time point, an aliquot was analyzed by radio-HPLC to assess radiochemical stability.

Determination of Albumin-binding Properties

The albumin-binding properties of CTT1401 and CTT1403 were determined using an ultrafiltration assay as previously described [34]. Briefly, centri-free ultrafiltration devices (Millipore, Billerica, MA) were used to separate the free CTT1401 or CTT1403 from the plasma protein-bound fraction. CTT1401 or CTT1403 (25 µL; 0.5 MBq) was added to 250 µL each of mouse and human serum (Sigma-Aldrich, St. Louis, MO). The mixtures were incubated at 37 °C for 15 min. As a negative control, the same procedure was performed using phosphate buffered saline instead of serum. After incubation, 250 µL of aliquots of the samples were loaded onto the ultrafiltration devices and centrifuged at 2500 rpm for 40 min in 20 °C, and 100 µL of each filtrate were counted in a gamma counter. The counts of the filtrate were calculated as a fraction of the radioactivity in the corresponding CTT1401 or CTT1403 solutions, which were set to 100%.

Biodistribution

Thirty NCr nude mice were injected with a 50:50 solution of saline and Matrigel (Corning, Corning, NY) (tumor injection solution) containing 1 × 10^6 PC3-PIP cells subcutaneously in the right shoulder. Tumors were allowed to grow until approximately 0.8 cm across (longest axis of measurement at 21 days post injection). Mice were injected via tail vein with 1.85 ± 0.07 MBq of CTT1401 or CTT1403 at a specific activity of 4 ± 3 MBq/nmol. Blocking was performed by pre-treating mice with 2-PMPA (442 nmol) 30 min prior to injection of CTT1401 or CTT1403. Animals were euthanized and tissues harvested at 1 h, 4 h, 4 h (blocked), 24 h, 48 h and 72 h post-injection. Because CTT1403 does not completely clear by 72 h like CTT1401, data for later biodistribution time points at 120 and 168 h were also collected. Blood, kidney, liver, lung, spleen, muscle, heart, bone, tumor, prostate, small intestine, large intestine, stomach and lacrimal glands were harvested. Tissue samples were counted in a gamma counter for 3 min each. Post-weights were taken to determine mass of tissue. Tissue weights and counts per minute (CPM) of Lu-177 were used to calculate biodistribution.

To assess specificity, 10 NCr male, nude mice were injected with a tumor injection solution containing 1 × 10^6 PC3-WT cells subcutaneously in the right shoulder. Tumors were allowed to grow until approximately 0.8 cm across (longest axis of measurement at 34 days post injection). Mice were injected with 1.85 ± 0.07 MBq of CTT1401 or CTT1403 tracer via tail vein at a specific activity of 4 ± 1 MBq/nmol. Animals were euthanized and tissues harvested at 4 and 24 h post-injection. Blood, kidney, liver, lung, spleen, muscle, heart, bone, tumor, prostate, small intestine, large intestine, stomach and lacrimal glands were harvested. Tissue samples were counted in a gamma counter for 3 min each. Post-harvest-weights were taken to determine mass of tissue. Tissue weights and CPM were used to calculate biodistribution.

In Vivo Targeted Radionuclide Therapy

NCr nude mice were injected with a tumor injection solution containing 3 × 10^5 PC3-PIP cells subcutaneously in the right shoulder 8 days before start of the therapy using CTT1401 (11 mice) or 10 days before start of the therapy using CTT1403 (8 mice). Average tumor volume at the start of treatment was 10-20 mm^3. Each mouse was injected with 29 ± 0.37 MBq of CTT1401 or CTT1403 via tail vein at a specific activity of 10 and 12 MBq/nmol, respectively. Control mice (7 in the CTT1401 experiment and 10 in the CTT1403 experiment) were injected with saline via tail vein. Body weights and tumor volumes were measured before injection at day 8 or 10 followed by measurements three times per week. The tumor volume (V) was determined according to the equation [V = (π ÷ 6) × L × W × H], where L is the longest axis and W is the perpendicular axis to L, and H is the perpendicular axis to L and W plane. Endpoint criteria were defined as when the longest axis of measurement of tumor exceeded 1.5 cm or there was active ulceration of the tumor. Survival curves were determined by the Kaplan-Meier method using the tumor implant day as day 0. Mouse weights were recorded throughout the survival period.

Statistics

Statistical analysis was performed using Prism 7 software (GraphPad, San Diego, CA). Biodistribution was assessed using unpaired two tailed t test. *P* values of less than or equal to 0.05 were considered significant. Survival analysis was performed with Kaplan-Meier curves and the Log-Rank Test.

Results

Synthesis and Radiochemistry

The preparation of the precursors CTT1400 and CTT1402 is fully detailed in the Supplemental Material (**Schemes S1 & S2, Figures S1-S6, Tables S1-S8**). Radiolabeling of the precursors was accomplished by first reacting ^{177}Lu-acetate with DOTA-N_3 followed by a click-chemistry step to assemble the intact CTT1401 and CTT1403 (**Scheme 1**). $^{177}LuCl_3$ and DOTA-N_3 were incubated in an ammonium acetate buffer (pH = 4.95) with gentisic acid at 95°C for 1 h. The DOTA-N_3 incorporated the ^{177}Lu-acetate readily with a radiochemical yield of >95% as determined by radio-HPLC with a specific activity up to 28 MBq/nmol. Subsequently, the copper-free click reaction was initiated by adding DBCO-bearing CTT1400 or CTT1402 into the ^{177}Lu-DOTA-N_3 mixture at 37 °C for 1 h. The higher concentration of CTT1400/1402 was essential to maximize the yield of the reaction in a timely manner at low temperature. The yields of CTT1401 and CTT1403 were found to be >95% as determined by radio-HPLC. The specific activities ranged from 6-7 MBq/nmol for CTT1401 and 1-3 MBq/nmol for CTT1403 in biodistribution studies and 10 MBq/nmol for CTT1401 and 12 MBq/nmol for CTT1403 in therapeutic efficacy studies. Serum stability *in vitro* showed that CTT1403 was >96% intact out to 24 h (**Figure S7A, B**). CTT1401 showed no binding to either mouse or human albumin, while CTT1403 bound ~90% to both species of albumin (**Figure S7C**). The binding of CTT1403 to mouse and human albumin are consistent with folate agents having the same albumin-binding moiety [33, 34].

Cellular Uptake and Internalization

CTT1401 and CTT1403 were rapidly incorporated in PC3-PIP cells within 15 min (25.6 ± 1.2 % injected dose (ID)/mg and 29.3 ± 1.2 %ID/mg, respectively) and steadily increased over 4 h, achieving 72.3 ± 0.9 %ID/mg and 86.0 ± 0.5 %ID/mg total uptake, respectively (**Figure 1**). Nearly 90% of the CTT1401 or CTT1403 bound to PC3-PIP cells was internalized within 2 h, and by 4 h 96.8 ± 0.3% and 99.2 ± 0.1% was internalized, respectively (**Table S9**). This followed trends observed previously with CTT1057 [15]. Blocking the PSMA active site with an excess of the competitive inhibitor 2-PMPA prior to the introduction of either agent prevented the binding of CTT1401 or CTT1403 (≤ 2 %ID/mg protein uptake at all time points). Non-specific uptake in PC3-WT cells was low (< 1 %ID/mg protein) for both agents. It is interesting to note that due to the reversible nature of the 2-PMPA inhibitor and the irreversible mode of inhibition of the CTT1298 core in both CTT1401 and CTT1403, 2-PMPA could be competed out by CTT1401 and CTT1403 over 2 h despite concentrations that were ~10,000-fold greater than CTT1401 or CTT1403 (data not shown).

Biodistribution

The results of the biodistribution of CTT1401 and CTT1403 in PC3-PIP tumor-bearing mice are shown in **Figures 2 and 3** and summarized in **Tables S10 and S11** (Supplementary Materials). Notable uptake of both CTT1401 and CTT1403 was observed for kidneys, lung, prostate, gastrointestinal tract, lacrimal glands, and PC3-PIP tumors. Without the albumin-binding scaffold, CTT1401 was rapidly cleared from blood (0.25 %ID/g at 1 h and ≤0.01 %ID/g in all later time points). CTT1401 uptake in PC3-PIP tumors peaked at 4 h and then decreased over 72 h (3.0 %ID/g at 4 h; 1.0 %ID/g at 72 h). In sharp contrast, CTT1403 exhibited prolonged blood circulation with gradual clearance (25 %ID/g at 1 h decreasing to 2.5 %ID/g at 72 h and 0.54% ID/g at 168 h). This pattern was observed in most organs other than kidney and the PC3-PIP tumors. Tumor uptake continued to increase over time (17 %ID/g at 4 h),

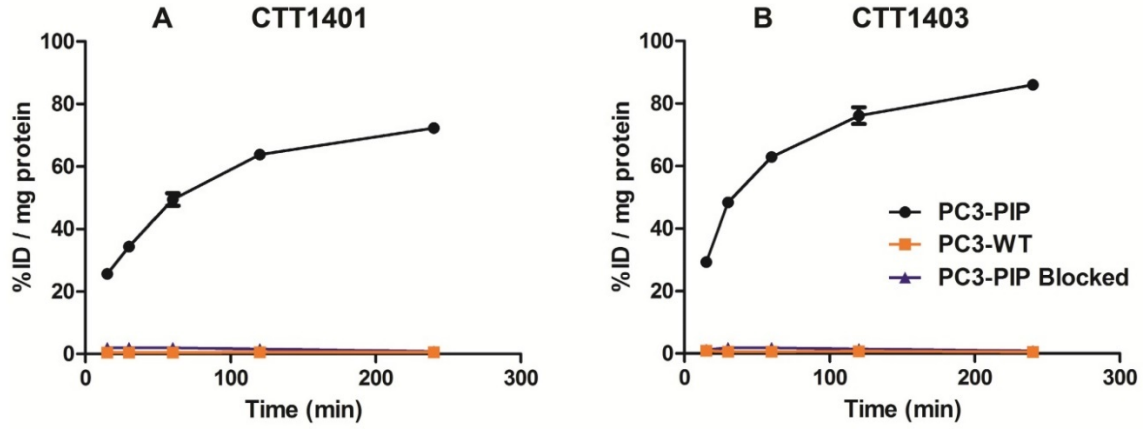

Figure 1. Uptake of CTT1401 (A) and CTT1403 (B) in PC3-PIP and PC3-WT cells.

reaching a maximum of 46 %ID/g at 72 h post injection. The tumor uptake of CTT1403 was substantially higher than CTT1401 at all time points (p = 0.0015 at 4 h and p < 0.001 at all other time points), and persisted out to 7 d post-injection, with >24 %ID/g in the tumor. Uptake of CTT1401 and CTT1403 were both PSMA-mediated, as a 30 min pre-injection of the U.S. Food and Drug Administration (FDA) approved reversible inhibitor 2-PMPA significantly decreased uptake of tracers in the kidneys and PC3-PIP tumors (**Figure 2B, D**; 3.0 %ID/g vs 1.1 %ID/g for CTT1401, p = 0.0012; 17.4 %ID/g vs 9.3 %ID/g for CTT1403, p = 0.041). Because 2-PMPA reversibly inhibits PSMA, it was not expected to completely block all specific PSMA dependent uptake by CTT1401 and CTT1403. Low to negligible uptake of both agents was observed in the PC3-WT tumors at 24 h post-injection (**Figure S8; Tables S10 and S12**) (2.11 %ID/g vs 0.01 %ID/g for CTT1401, 37.7 %ID/g vs 4.5 %ID/g for CTT1403).

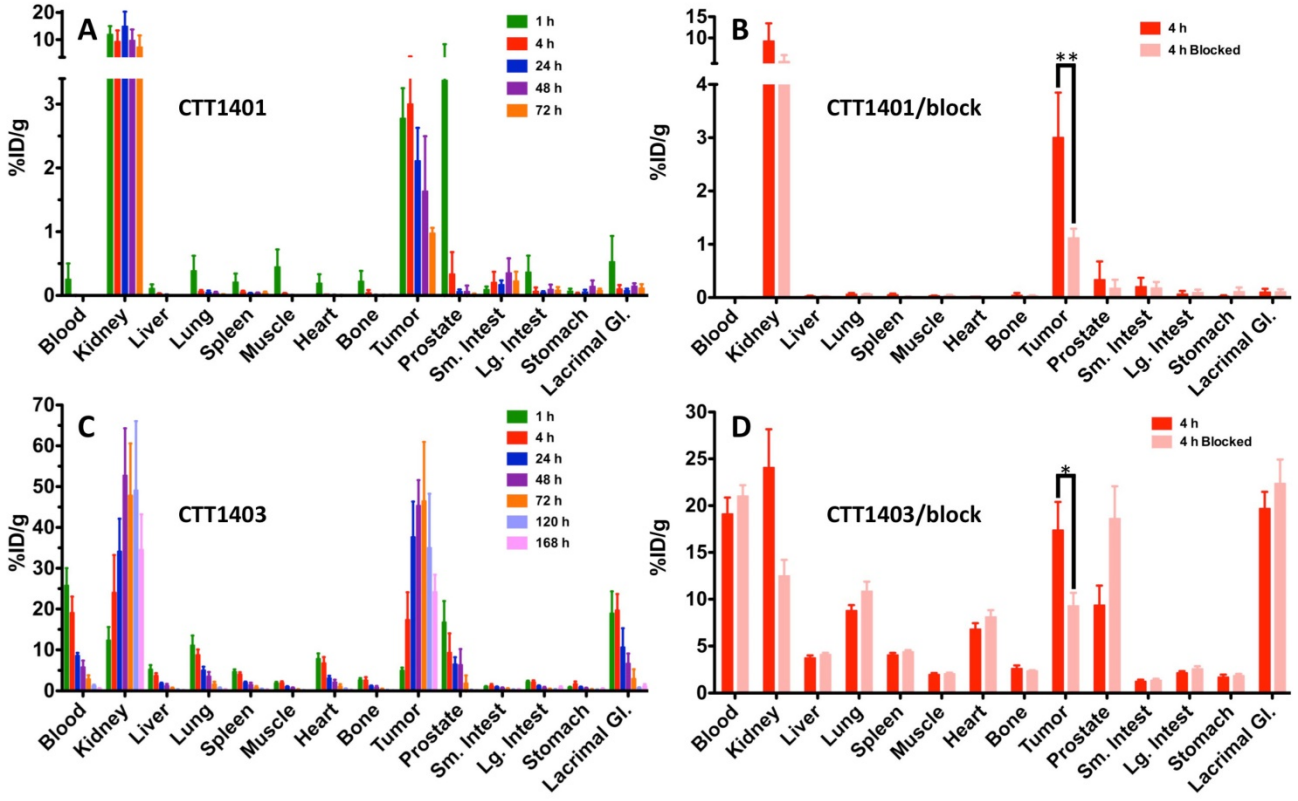

Figure 2. Biodistribution of ^{177}Lu-labeled CTT1401 (**A, B**) and CTT1403 (**C, D**) in PC3-PIP tumor-bearing mice. Pre-injection of 2-PMPA 30 min prior to the ^{177}Lu-labeled agents showed significant decreases in tumor and kidney. Data are presented as % injected dose per gram of tissue (n=5 per group, except n=10 for CTT1403 72 h group; mean +/- sd).

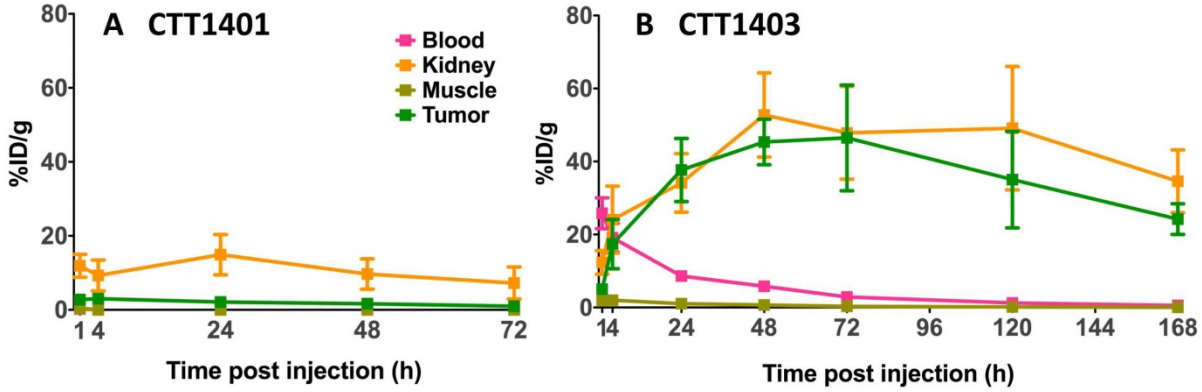

Figure 3. Biodistribution of ^{177}Lu-labeled CTT1401 (**A**) and CTT1403 (**B**) in in key PSMA+ (tumor, kidneys) and non-target tissues (blood, muscle) at 1, 4, 24, 28 and 72 h showing uptake and clearance. Data are presented as % injected dose per gram of tissue (n=5 per group, except n=10 for CTT1403 72 h group; mean +/- sd).

CTT1401 showed impressive tumor:non-tumor ratios, with tumor:blood peaking at 4 h (300 ± 84) and tumor:muscle reaching 211 ± 52 at 24 h post-injection (**Figure 4A, E**). Tumor:kidney ratios were 0.2-0.4 or lower at all time points (**Figure 4C**). In contrast, due to the slower blood clearance attributable to the albumin binding motif, the tumor:blood and tumor:muscle for CTT1403 is on the rise even at 168 h post-injection (**Figure 4B, F**). Tumor:kidney ratios are consistently between 0.7-1 after 4 h (**Figure 4D**). For both CTT1401 and CTT1403, the tumor:blood ratios were significantly lower upon blocking with 2-PMPA and in the PC3-WT tumor (**Figure 4G, H**). Together, the biodistribution and tumor:non-tumor ratio data showing slower clearing of CTT1403 and high retention in PC3-PIP tumors, underscore its attractiveness for PSMA-targeted therapy.

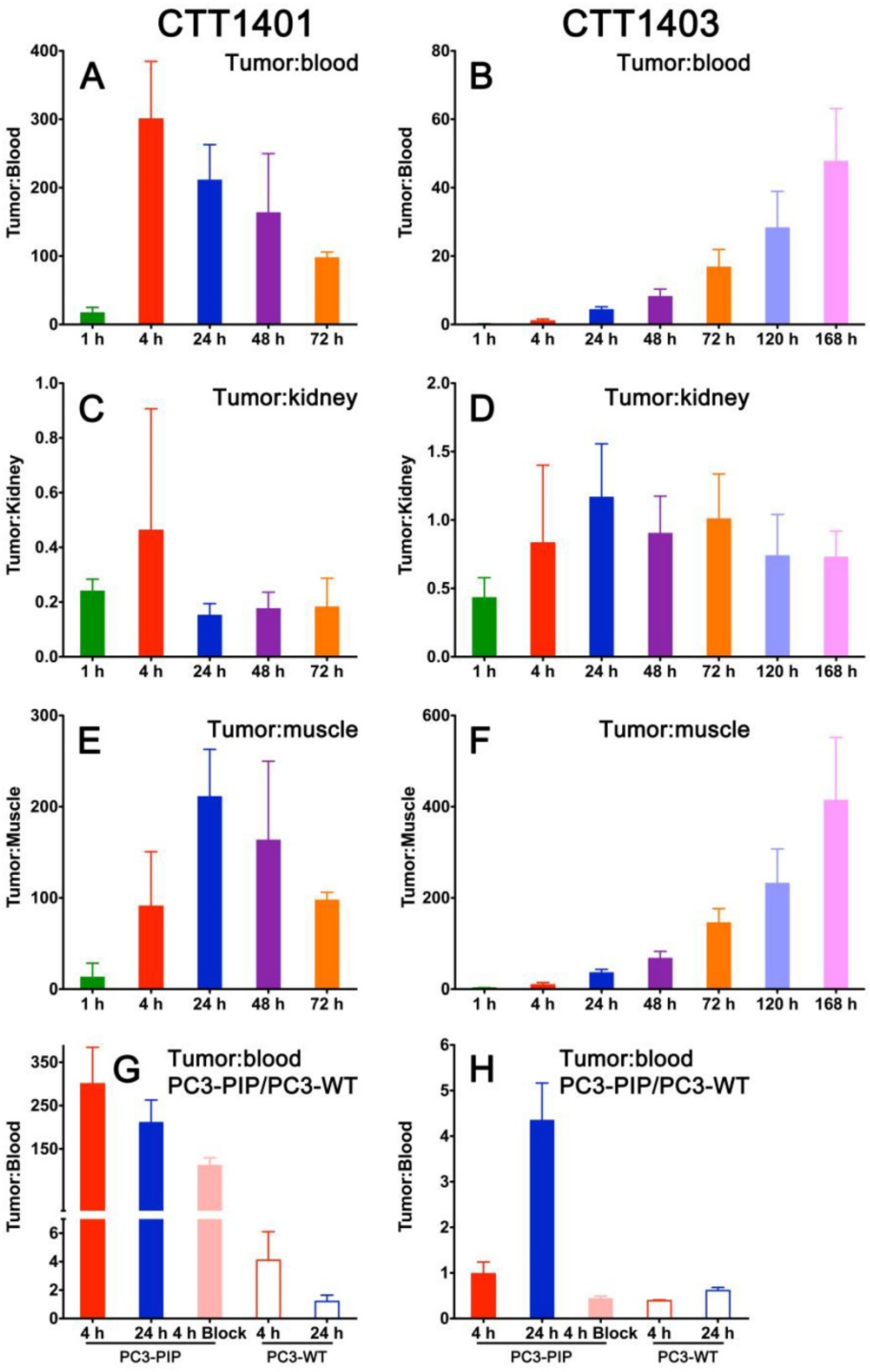

Figure 4. Tumor:non-tumor ratios for CTT1401 (**panels A, C, E, G**) and CTT1403 (**panels B, D, F, H**) in PC3-PIP tumor-bearing mice. (n=5 per group, except n=10 for CTT1403 72 h group; mean +/- sd).

Therapeutic Efficacy

Animals were injected with a single dose of 29 MBq CTT1401/CTT1403, or saline (control group) approximately 7-10 days post-implantation of the tumor xenografts. After 14 weeks post tumor implant, only one mouse out of eight that received CTT1403 treatment had met the endpoint criteria for tumor growth (1.5 cm on the longest axis and/or tumor ulceration). In sharp contrast, all mice in the control and CTT1401 treatment groups reached their end point criteria within 8 weeks after receiving tumor implant. Minimal tumor growth inhibition was found in the CTT1401 treatment group, which had a median survival time of 47 days compared to 42 days for the control group (p = 0.45). Survival rates of CTT1403 group were statistically greater than the other groups (p < 0.0001, **Figure 5**), with median survival time of the CTT1403 mice not yet reached at 120 days. It is important to note that in all groups of mice, their weights remained constant or increased during the survival period (**Figure S9**) and there were no overt signs of toxicity (scruffy coat, diarrhea, lethargy). We therefore believe that a single dose of 29 MBq is below the maximum tolerated dose (MTD) in immune-compromised nude mice. Studies to determine the MTD are planned.

Discussion

PSMA-targeted Lu-177 radionuclide therapy has shown great promise, most recently in human clinical trials. The antibody J591 chelated with Lu-177 has been tested with moderate success, but shortcomings included an excessive circulation time that limited the therapeutic dose that could be delivered. It was found that myelosuppression was dose limiting for both single and repeat dosing of ^{177}Lu-J591. In terms of circulation time, whole-body retention of ^{177}Lu-J591 was ~70% 6 d after injection, and the half-life for clearance from the blood was approximately 44 h, with myelosuppression being dose limiting [2, 35]. In addition, liver uptake was considerable [36]. In contrast, clinical responses between 31-68% have been observed in initial trials with the reversible small-molecule ^{177}Lu-PSMA-617 with relatively low incidence of hematologic toxicity [29, 37, 38]. Although the early human data are promising, short circulation time is a disadvantage for these small-molecule radiotherapies, particularly with respect to the 6.7-day half-life of Lu-177. As a means to improve current radionuclide therapy approaches, we investigated the impact of small-molecule residence time by constructing and comparing two variations of the irreversible PSMA targeting small-molecule: CTT1401 and an analog, CTT1403, that includes an albumin binding moiety to improve circulation time. By extending circulation half-life of the targeted radiotherapeutic, the goal is to increase tumor:non-target ratios for PSMA expressing normal organs, such as kidneys, lacrimal glands, and salivary glands. This would likely then decrease the amount of ^{177}Lu-labeled PSMA agent required for efficacy and decrease toxicity to normal tissues. There is precedence for this with the ^{177}Lu-cm09, which showed decreased folate receptor-mediated kidney uptake and lower kidney dose compared to the same compound minus an albumin binding domain [39].

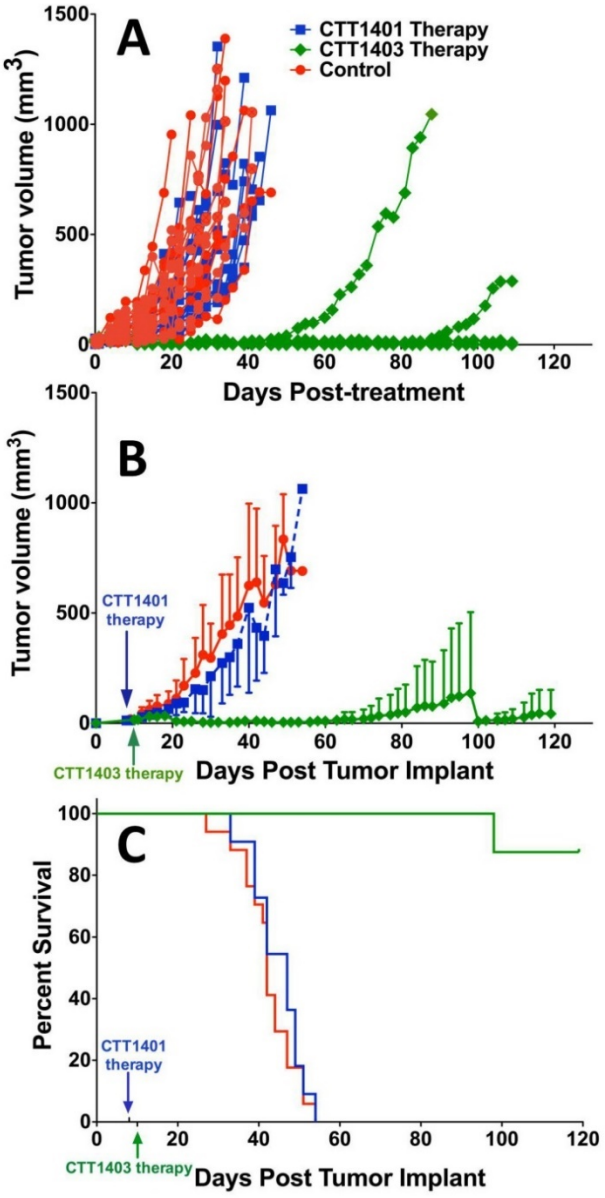

Figure 5. Therapeutic efficacy of CTT1401 and CTT1403. (**A**) Comparison of the therapeutic efficacy in the mice groups treated with a single dose of CTT1401 or CTT1403 in comparison to the control group (untreated). (**B**) Average tumor growth for mice treated with a single dose of CTT1401 or CTT1403 in comparison to the control group (untreated). (**C**) Survival data for mice treated with a single dose of CTT1401 or CTT1403 in comparison to the control group (untreated).

Irreversible inhibitors offer persistent target binding after the drug has been cleared. This translates to a longer lasting duration of drug action at the target site over the reversible inhibitors [40]. This feature is particularly desirable for targeted radiotherapy using longer half-lived radionuclides, allowing the radioactivity to remain in the target, maximizing the therapeutic effect while minimizing off-target side effects. The more efficient dose utilization may facilitate the reduction of dose or dosing frequency.

The design of the CTT1401 and CTT1403 structures are based on the successful PSMA-targeting molecule CTT1298, which is a known irreversible inhibitor of PSMA [14, 15]. This class of phosphoramidate inhibitors has been shown to not only exhibit high affinity for PSMA, but to rapidly and selectively penetrate PSMA positive cells through the internalization of the PSMA enzyme-inhibitor complex [41-43]. Like the urea-based reversible PSMA inhibitors, these phosphoramidate-based PSMA inhibitor scaffolds are capable of delivering a diverse array of payloads ranging from imaging radionuclides to small fluorescent dyes to complexes with streptavidin or therapeutic enzymes [14-16, 41-53]. Most recently, CTT1298 was used to prepare the PSMA-targeted PET imaging agent CTT1057 by conjugating it with [^{18}F]-4-fluorobenzoate (SFB) [14, 15]; CTT1057 recently entered a Phase I PET imaging clinical trial and would be the candidate for a companion diagnostic for CTT1403, should CTT1403 proceed to human studies.

The objective of this study was to determine the effect of the albumin-binding motif on the biodistribution, and ultimately the therapeutic efficacy, of CTT1298-based radionuclide therapy agents. The radiolabeling precursor CTT1402 required the installation of the albumin-binding motif, which was combined with the DBCO-PEG$_4$-NHS prior to coupling to CTT1298. In both cases, the click-ready DBCO group afforded a radiolabeling precursor that could be conveniently combined with the ^{177}Lu-complexed DOTA-N$_3$ through copper-free click chemistry to form the intact PSMA-targeted radiotherapeutic agents. The two-step approach to preparing CTT1401 and CTT1403 was needed because of the sensitivity of the phosphoramidate P-N bond at the center of the PSMA-binding moiety to low pH, especially at elevated temperatures. An additional advantage to this process is the flexibility to installing alternative payloads onto CTT1400/1402 platform. For the studies presented here, an HPLC purification step was included to purify CTT1401 and CTT1403 from unreacted CTT1400 and CTT1402, for a total preparation time of about 2 h. We are currently optimizing the purification of CTT1403 from unreacted CTT1402 using a solid-phase resin, which will eliminate the HPLC purification step as well as shorten the production time. The two-step radiolabeling process was performed in one pot in order to maximize radiochemical yield and minimize radiolysis. The formation of ^{177}Lu-DOTA complexes requires a specific environment of pH 4.0–4.5 [54]. Fortunately, the use of the subsequent strain-promoted [3+2] cycloaddition (i.e., click chemistry reaction) with the radiolabeling precursors is versatile through a wide pH range with high chemoselectivity, eliminating the need to isolate the ^{177}Lu-DOTA intermediate to accommodate the second reaction. Finally, the desired PSMA-targeted radiotherapeutic agent was isolated from the reaction mixture using HPLC and stabilized with a cocktail of gentisic acid, sodium ascorbate and ethanol [55-57].

The blood circulation time of CTT1403 was significantly extended from CTT1401 after installation of 4-(p-iodophenyl)butyric acid, a small molecule that binds to both mouse and human serum albumin with a dissociation constant of 3.6 and 3.2 μM, respectively [32]. Previously, this structure was successfully conjugated to either antibody fragments [58] or small molecule (^{177}Lu-cm09) [33], leading to extended serum half-life and increased tumor uptake. To our knowledge, this is the first example of adding an albumin-binding entity to a PSMA-targeted radiotherapeutic agent. More recently, Chen *et al.* showed that truncated Evans Blue dyes prolong circulation and increase tumor uptake in αvβ3-expressing tumors [59]. The use of the 4-(p-iodophenyl)butyric acid based albumin-binding motif, united with the irreversible phosphoramidate based PSMA binding core on CTT1403, resulted in retention of tumor uptake for at least 7 days, which is unusual for PSMA-targeted small-molecule agents. Indeed, this behavior is markedly different from that of CTT1401, which exhibited a similarly rapid clearance profile to that of other small-molecule PSMA inhibitors. The slow and steady clearance of CTT1403 was attributed to the known binding of the 4-(p-iodophenyl)butyryl group to albumin resulting in extended exposure of CTT1403 to PSMA on target cells. Additionally, the tumor:kidney ratio of CTT1403 is 0.7-1, whereas previously published data for ^{177}Lu-PSMA I&T show kidney uptake of >100%ID/g and tumor:kidney ratios between 0.1-0.3 [60], similar to CTT1401.

While it is known that drug uptake in tumors through the enhanced permeation and retention (EPR) effect can be improved by albumin binding [61, 62], outfitting small-molecule PSMA inhibitors with specific albumin binding motifs has not been reported

previously. In addition, there is a paucity of reports on *in vitro* tracer uptake data for small-molecule PSMA-targeted radiotherapeutic agents in the literature for comparison, specifically using the PC3-PIP cell line. Kiess *et al.*, using an alpha-emitting ^{211}At-labeled urea-based PSMA-inhibitor scaffold, demonstrated PIP-PC3 uptake averaging ~28% input dose [63]. The CTT1403 scaffold achieved 85.4 ± 0.50 % input dose under the same timeframe with this cell line (**Figure 1**), while maintaining a similar blocked and non-specific uptake profile. For both CTT1401 and CTT1403, the ratio of internalized to total uptake was 96.8 ± 0.34 and 99.2 ± 0.17, respectively (**Table S9**). Interestingly, similar data are not reported for the At-211 agent, where internalization of this alpha emitter would be of great relevance.

The PSMA-mediated PC3-PIP tumor uptake for CTT1403 *in vivo*, which peaks at ~46%ID/g at 72 h, is uncharacteristically high for radiolabeled PSMA inhibitors. Although kidney uptake is prominent for both compounds, the tumor-to-kidney ratios for CTT1403 are 2-4 fold higher than CTT1401 at all time points. This is consistent with literature data showing that addition of albumin-binding entity comes with the benefit of enhanced tumor:kidney ratio [33, 39, 64]. The biodistribution of CTT1403 showed a tumor:kidney ratio of ~1 at time points longer than 4 h. For comparison, for the ^{211}At-labeled urea-based agent, the kidney uptake was 3-4 fold greater than that of the tumor, and long-term toxicity studies confirmed that the high kidney uptake was dose-limiting [63]. For PSMA-targeted therapy, co-administration of 2-PMPA is a documented strategy to improve the tumor:kidney ratio [60, 65] and may effectively complement the addition of the albumin-binding moiety as shown in our blocking study. Chatalic *et al.* compared therapy with 100 MBq of ^{177}Lu-PSMA I&T (29 MBq CTT1403 was used in this study) with and without 2-PMPA in PSMA-transfected LS174T colorectal tumor-bearing mice. Median survival was 19 d and 29 d for ^{177}Lu-PSMA I&T with and without 2-PMPA, respectively (compared to 13 d for controls), indicating that the decrease in tumor uptake due to 2-PMPA led to decreased efficacy, although the tumor:kidney ratio increased by a factor of ~2. It should be noted that unlike human kidney, rodent kidney demonstrates substantial levels of PSMA expression and kidney clearance kinetics is somewhat obscured by this specific PSMA uptake [23, 66-69].

The slow clearance of CTT1403 is well matched to the longer half-life of Lu-177 for therapeutic purposes, and the enhanced tumor uptake observed in the biodistribution studies for CTT1403 translated into superior therapeutic efficacy (**Figure 5**). Despite a slight increase in tumor volume in the first two weeks, a single dose of CTT1403 generally suppressed tumor growth for over 14 weeks. After 100 days (ten half-lives of ^{177}Lu), only one mouse in the CTT1403 treatment group met the endpoint criteria, while one mouse had a tumor exhibiting signs of growth. In fact, all tumors in this treatment group were less than 25 mm^3 in volume at 56 days post-tumor implant, while all mice in the control group or the CTT1401 treatment group had met the endpoint criteria. While CTT1401 exhibited typical biodistribution and clearance kinetics for PSMA-targeted small-molecules, no significant tumor growth inhibition was observed in the CTT1401 treatment group.

For a single dose of 740 kBq of a ^{211}At-labeled PSMA-targeted agent in the PC3-PIP mouse model, the median time to reach 10-fold tumor volume for animals treated with the radiotherapy was 35 days, which was significantly longer than the 19 days of the untreated group [63]. Although 80% of the PC3-PIP tumor-bearing mice were sacrificed by day 45, 20% survived over 200 days. One dose of 29 MBq CTT1403 imparted survival of 90% of mice beyond 120 days, compared with a median survival of 42 days for saline controls. Although CTT1403 was not directly compared to the ^{211}At-labeled agent, the biodistribution of CTT1403 suggests an advantage for the irreversible PSMA inhibitor in combination with an albumin-binding motif.

Conclusions

With the objective of identifying a PSMA-targeted radiotherapeutic candidate to advance to manufacturing and IND-enabling studies, we compared two phosphoramidate-based scaffolds, which differed with respect to possessing an albumin-binding motif. The albumin binding moiety in CTT1403 confers clear advantages to the PSMA-inhibitor scaffold including increased circulating half-life and prostate tumor uptake that continued to increase up to 48-72 h post injection. This increased tumor uptake translated into superior therapeutic efficacy of CTT1403 in PSMA+ human xenograft tumor models as demonstrated by significantly increased tumor doubling times, 90-95% reduction in tumor volume within the first 3 weeks of tumor growth, and a median survival time that exceeded 120 days. CTT1403 also demonstrated improved clearance kinetics as compared to CTT1401 and other small-molecule PSMA ligands. The preparation of the radiolabeling precursor, CTT1402, involves more synthetic steps than CTT1400; however, the markedly superior therapeutic performance of CTT1403 outweighs the additional complexity to produce the molecule. CTT1403 will

shortly undergo IND-enabling pharmacology studies to assess dose, regimen, estimated human dosimetry, and safety studies.

Supplementary Material

Experimental procedures and characterization data for CTT1400 and CTT1402, Supplementary figures and tables. http://www.thno.org/v07p1928s1.pdf

Abbreviations

PSMA: prostate-specific membrane antigen; I&T: imaging and therapy; DOTA: 1,4,7,10-tetraazacyclo-dodecane-1,4,7,10-tetraacetic acid; PET: positron emission tomography; DBCO: dibenzocyclooctyne; IACUC: Institutional Animal Care and Use Committee; HPLC: high performance liquid chromatography; FBS: Fetal Bovine Serum; 2-PMPA: 2-(Phosphonomethyl)pentane-1,5-dioicacid; HBSS: Hank's Balanced Salt Solution; SDS: sodium dodecyl sulfate; $_{dd}H_2O$: double distilled water; BSA: Bovine serum albumin; CPM: counts per minute; V: tumor volume; ID: injected dose; FDA: U.S. Food and Drug Administration; SFB: 4-fluorobenzoate; PEG: polyethylene glycol; NHS: *N*-hydroxysuccinimide; EPR: enhanced permeation and retention; IND: Investigational New Drug; WSU: Washington State University

Acknowledgements

This work was supported by a contract from the National Institutes of Health (HHSN261201500074C) and a grant from the Department of Energy (DE-SC0008833) for partial support of Drs. Geruntho and Ling. University of Pittsburgh Cancer Institute shared resources (In Vivo Imaging Facility) were used in this research and supported in part by NCI P30CA047904. The authors extend their gratitude for technical assistance to G. Helms and W. Hiscox (Washington State University (WSU) Center for Nuclear Magnetic Resonance Spectroscopy) and Gerhard Munske (WSU Laboratory of Biotechnology and Bioanalysis).

Competing Interests

Dr. Langton-Webster serves as the Chief Executive Officer for Cancer Targeted Technology. Dr. Berkman serves at the Chief Science Officer for Cancer Targeted Technology and is the inventor of the CTT1298 PSMA inhibitor scaffold.

References

1. Rosenthal SA, Haseman MK, Polascik TJ. Utility of capromab pendetide (ProstaScint) imaging in the management of prostate cancer. Tech Urol. 2001; 7: 27-37.
2. Bander NH, Milowsky MI, Nanus DM, Kostakoglu L, Vallabhajosula S, Goldsmith SJ. Phase I trial of 177lutetium-labeled J591, a monoclonal antibody to prostate-specific membrane antigen, in patients with androgen-independent prostate cancer. J Clin Oncol. 2005; 23: 4591-601.
3. Chu TC, Shieh F, Lavery LA, Levy M, Richards-Kortum R, Korgel BA, et al. Labeling tumor cells with fluorescent nanocrystal-aptamer bioconjugates. Biosens Bioelectron. 2006; 21: 1859-66.
4. Farokhzad OC, Khademhosseini A, Jon S, Hermmann A, Cheng J, Chin C, et al. Microfluidic system for studying the interaction of nanoparticles and microparticles with cells. Anal Chem. 2005; 77: 5453-9.
5. Foss CA, Mease RC, Fan H, Wang Y, Ravert HT, Dannals RF, et al. Radiolabeled small-molecule ligands for prostate-specific membrane antigen: in vivo imaging in experimental models of prostate cancer. Clin Cancer Res. 2005; 11: 4022-8.
6. Gao X, Cui Y, Levenson RM, Chung LW, Nie S. In vivo cancer targeting and imaging with semiconductor quantum dots. Nat Biotechnol. 2004; 22: 969-76.
7. Guilarte TR, McGlothan JL, Foss CA, Zhou J, Heston WD, Kozikowski AP, et al. Glutamate carboxypeptidase II levels in rodent brain using [125I]DCIT quantitative autoradiography. Neuroscience letters. 2005; 387(3): 141-4.
8. Humblet V, Lapidus R, Williams LR, Tsukamoto T, Rojas C, Majer P, et al. High-affinity near-infrared fluorescent small-molecule contrast agents for in vivo imaging of prostate-specific membrane antigen. Mol Imaging. 2005; 4: 448-62.
9. Milowsky MI, Nanus DM, Kostakoglu L, Sheehan CE, Vallabhajosula S, Goldsmith SJ, et al. Vascular targeted therapy with anti-prostate-specific membrane antigen monoclonal antibody J591 in advanced solid tumors. J Clin Oncol. 2007; 25: 540-7.
10. Pomper MG, Musachio JL, Zhang J, Scheffel U, Zhou Y, Hilton J, et al. 11C-MCG: synthesis, uptake selectivity, and primate PET of a probe for glutamate carboxypeptidase II (NAALADase). Mol Imaging. 2002; 1: 96-101.
11. Smith MR, Nelson JB. Future therapies in hormone-refractory prostate cancer. Urology. 2005; 65: 9-16.
12. Smith-Jones PM, Vallabhajosula S, Navarro V, Bastidas D, Goldsmith SJ, Bander NH. Radiolabeled monoclonal antibodies specific to the extracellular domain of prostate-specific membrane antigen: preclinical studies in nude mice bearing LNCaP human prostate tumor. J Nucl Med. 2003; 44: 610-7.
13. Tsukamoto T, Wozniak KM, Slusher BS. Progress in the discovery and development of glutamate carboxypeptidase II inhibitors. Drug Discov Today. 2007; 12: 767-76.
14. Ganguly T, Dannoon S, Hopkins MR, Murphy S, Cahaya H, Blecha JE, et al. A high-affinity [(18)F]-labeled phosphoramidate peptidomimetic PSMA-targeted inhibitor for PET imaging of prostate cancer. Nucl Med Biol. 2015; 42: 780-7.
15. Dannoon S, Ganguly T, Cahaya H, Geruntho JJ, Galliher MS, Beyer SK, et al. Structure-Activity Relationship of (18)F-Labeled Phosphoramidate Peptidomimetic Prostate-Specific Membrane Antigen (PSMA)-Targeted Inhibitor Analogues for PET Imaging of Prostate Cancer. J Med Chem. 2016; 59: 5684-94.
16. Nedrow JR, Latoche JD, Day KE, Modi J, Ganguly T, Zeng D, et al. Targeting PSMA with a Cu-64 Labeled Phosphoramidate Inhibitor for PET/CT Imaging of Variant PSMA-Expressing Xenografts in Mouse Models of Prostate Cancer. Mol Imaging Biol. 2016; 18: 402-10.
17. Tasch J, Gong M, Sadelain M, Heston WD. A unique folate hydrolase, prostate-specific membrane antigen (PSMA): a target for immunotherapy? Crit Rev Immunol. 2001; 21: 249-61.
18. Salit RB, Kast WM, Velders MP. Ins and outs of clinical trials with peptide-based vaccines. Front Biosci. 2002; 7: e204-13.
19. Lu J, Celis E. Recognition of prostate tumor cells by cytotoxic T lymphocytes specific for prostate-specific membrane antigen. Cancer Res. 2002; 62: 5807-12.
20. Fracasso G, Bellisola G, Cingarlini S, Castelletti D, Prayer-Galetti T, Pagano F, et al. Anti-tumor effects of toxins targeted to the prostate specific membrane antigen. Prostate. 2002; 53: 9-23.
21. Ghosh A, Heston WD. Tumor target prostate specific membrane antigen (PSMA) and its regulation in prostate cancer. J Cell Biochem. 2004; 91: 528-39.
22. Murphy GP, Su S, Jarisch J, Kenny GM. Serum levels of PSMA. Prostate. 2000; 42: 318-9.
23. Bacich DJ, Pinto JT, Tong WP, Heston WD. Cloning, expression, genomic localization, and enzymatic activities of the mouse homolog of prostate-specific membrane antigen/NAALADase/folate hydrolase. Mamm Genome. 2001; 12: 117-23.
24. Chang SS, O'Keefe DS, Bacich DJ, Reuter VE, Heston WD, Gaudin PB. Prostate-specific membrane antigen is produced in tumor-associated neovasculature. Clin Cancer Res. 1999; 5(10): 2674-81.
25. Chang SS, Reuter VE, Heston WD, Gaudin PB. Comparison of anti-prostate-specific membrane antigen antibodies and other immunomarkers in metastatic prostate carcinoma. Urology. 2001; 57: 1179-83.
26. Weineisen M, Schottelius M, Simecek J, Baum RP, Yildiz A, Beykan S, et al. 68Ga- and 177Lu-Labeled PSMA I&T: Optimization of a PSMA-Targeted Theranostic Concept and First Proof-of-Concept Human Studies. J Nucl Med. 2015; 56: 1169-76.
27. Baum RP, Kulkarni HR, Schuchardt C, Singh A, Wirtz M, Wiessalla S, et al. 177Lu-Labeled Prostate-Specific Membrane Antigen Radioligand Therapy of Metastatic Castration-Resistant Prostate Cancer: Safety and Efficacy. J Nucl Med. 2016; 57: 1006-13.
28. Rahbar K, Bode A, Weckesser M, Avramovic N, Claesener M, Stegger L, et al. Radioligand Therapy With 177Lu-PSMA-617 as A Novel Therapeutic Option

in Patients With Metastatic Castration Resistant Prostate Cancer. Clin Nucl Med. 2016; 41: 522-8.
29. Ahmadzadehfar H, Rahbar K, Kurpig S, Bogemann M, Claesener M, Eppard E, et al. Early side effects and first results of radioligand therapy with (177)Lu-DKFZ-617 PSMA of castrate-resistant metastatic prostate cancer: a two-centre study. EJNMMI Res. 2015; 5: 114.
30. Kwekkeboom D. Perspective on 177Lu-PSMA Therapy for Metastatic Castration-Resistant Prostate Cancer. J Nucl Med. 2016; 57: 1002-3.
31. Liu Z, Chen X. Simple bioconjugate chemistry serves great clinical advances: albumin as a versatile platform for diagnosis and precision therapy. Chem Soc Rev. 2016; 45: 1432-56.
32. Dumelin CE, Trussel S, Buller F, Trachsel E, Bootz F, Zhang Y, et al. A portable albumin binder from a DNA-encoded chemical library. Angew Chem Int Ed Engl. 2008; 47: 3196-201.
33. Muller C, Struthers H, Winiger C, Zhernosekov K, Schibli R. DOTA conjugate with an albumin-binding entity enables the first folic acid-targeted 177Lu-radionuclide tumor therapy in mice. J Nucl Med. 2013; 54: 124-31.
34. Siwowska K, Haller S, Bortoli F, Benesova M, Groehn V, Bernhardt P, et al. Preclinical Comparison of Albumin-Binding Radiofolates: Impact of Linker Entities on the in Vitro and in Vivo Properties. Mol Pharm. 2017; 14: 523-32.
35. Vallabhajosula S, Goldsmith SJ, Kostakoglu L, Milowsky MI, Nanus DM, Bander NH. Radioimmunotherapy of prostate cancer using 90Y- and 177Lu-labeled J591 monoclonal antibodies: effect of multiple treatments on myelotoxicity. Clin Cancer Res. 2005; 11: 7195s-200s.
36. Vallabhajosula S, Kuji I, Hamacher KA, Konishi S, Kostakoglu L, Kothari PA, et al. Pharmacokinetics and biodistribution of 111In- and 177Lu-labeled J591 antibody specific for prostate-specific membrane antigen: prediction of 90Y-J591 radiation dosimetry based on 111In or 177Lu? J Nucl Med. 2005; 46: 634-41.
37. Yadav MP, Ballal S, Tripathi M, Damle NA, Sahoo RK, Seth A, et al. 177Lu-DKFZ-PSMA-617 therapy in metastatic castration resistant prostate cancer: safety, efficacy, and quality of life assessment. Eur J Nucl Med Mol Imaging. 2017; 44: 81-91.
38. Rahbar K, Schmidt M, Heinzel A, Eppard E, Bode A, Yordanova A, et al. Response and Tolerability of a Single Dose of 177Lu-PSMA-617 in Patients with Metastatic Castration-Resistant Prostate Cancer: A Multicenter Retrospective Analysis. J Nucl Med. 2016; 57: 1334-8.
39. Haller S, Reber J, Brandt S, Bernhardt P, Groehn V, Schibli R, et al. Folate receptor-targeted radionuclide therapy: preclinical investigation of anti-tumor effects and potential radionephropathy. Nucl Med Biol. 2015; 42: 770-9.
40. Singh J, Petter RC, Baillie TA, Whitty A. The resurgence of covalent drugs. Nat Rev Drug Discov. 2011; 10: 307-17.
41. Nedrow-Byers JR, Moore AL, Ganguly T, Hopkins MR, Fulton MD, Benny PD, et al. PSMA-targeted SPECT agents: mode of binding effect on in vitro performance. Prostate. 2013; 73: 355-62.
42. Nedrow-Byers JR, Jabbes M, Jewett C, Ganguly T, He H, Liu T, et al. A phosphoramidate-based prostate-specific membrane antigen-targeted SPECT agent. Prostate. 2012; 72: 904-12.
43. Liu T, Wu LY, Kazak M, Berkman CE. Cell-Surface labeling and internalization by a fluorescent inhibitor of prostate-specific membrane antigen. Prostate. 2008; 68: 955-64.
44. Lapi SE, Wahnishe H, Pham D, Wu LY, Nedrow-Byers JR, Liu T, et al. Assessment of an 18F-labeled phosphoramidate peptidomimetic as a new prostate-specific membrane antigen-targeted imaging agent for prostate cancer. J Nucl Med. 2009; 50: 2042-8.
45. Liu T, Jabbes M, Nedrow-Byers JR, Wu LY, Bryan JN, Berkman CE. Detection of prostate-specific membrane antigen on HUVECs in response to breast tumor-conditioned medium. Int J Oncol. 2011; 38: 1349-55.
46. Liu T, Nedrow-Byers JR, Hopkins MR, Berkman CE. Spacer length effects on in vitro imaging and surface accessibility of fluorescent inhibitors of prostate specific membrane antigen. Bioorg Med Chem Lett. 2011; 21: 7013-6.
47. Liu T, Wu LY, Berkman CE. Prostate-specific membrane antigen-targeted photodynamic therapy induces rapid cytoskeletal disruption. Cancer Lett. 2010; 296: 106-12.
48. Liu T, Wu LY, Choi JK, Berkman CE. In vitro targeted photodynamic therapy with a pyropheophorbide--a conjugated inhibitor of prostate-specific membrane antigen. Prostate. 2009; 69: 585-94.
49. Liu T, Wu LY, Choi JK, Berkman CE. Targeted photodynamic therapy for prostate cancer: inducing apoptosis via activation of the caspase-8/-3 cascade pathway. Int J Oncol. 2010; 36: 777-84.
50. Liu T, Wu LY, Hopkins MR, Choi JK, Berkman CE. A targeted low molecular weight near-infrared fluorescent probe for prostate cancer. Bioorg Med Chem Lett. 2010; 20: 7124-6.
51. Wu LY, Liu T, Grimm AL, Davis WC, Berkman CE. Flow cytometric detection of prostate tumor cells using chemoaffinity labels. Prostate. 2011; 71: 52-61.
52. Lee J, Chen H, Liu T, Berkman CE, Reilly PT. High resolution time-of-flight mass analysis of the entire range of intact singly-charged proteins. Anal Chem. 2011; 83: 9406-12.
53. Martin SE, Ganguly T, Munske GR, Fulton MD, Hopkins MR, Berkman CE, et al. Development of inhibitor-directed enzyme prodrug therapy (IDEPT) for prostate cancer. Bioconjug Chem. 2014; 25: 1752-60.
54. Breeman WA, De Jong M, Visser TJ, Erion JL, Krenning EP. Optimising conditions for radiolabelling of DOTA-peptides with 90Y, 111In and 177Lu at high specific activities. Eur J Nucl Med Mol Imaging. 2003; 30: 917-20.
55. A.P. Breeman W, Sze Chan H, M.S. de Zanger R, K. Konijnenberg M, de Blois E. Overview of Development and Formulation of 177Lu-DOTA-TATE for PRRT. Curr Rad. 2016; 9: 8-18.
56. Maus S, Blois ED, Ament SJ, Schreckenberger M, Breeman WAP. Aspects on radiolabeling of 177Lu-DOTA-TATE: After C18 purification re-addition of ascorbic acid is required to maintain radiochemical purity. IJDI. 2014; 1.
57. de Blois E, Chan HS, de Zanger R, Konijnenberg M, Breeman WA. Application of single-vial ready-for-use formulation of 111In- or 177Lu-labelled somatostatin analogs. Appl Radiat Isot. 2014; 85: 28-33.
58. Trussel S, Dumelin C, Frey K, Villa A, Buller F, Neri D. New strategy for the extension of the serum half-life of antibody fragments. Bioconjug Chem. 2009; 20: 2286-92.
59. Chen H, Jacobson O, Niu G, Weiss I, Kiesewetter DO, Liu Y, et al. Novel molecular "add-on" based on Evans Blue confers superior pharmacokinetics and transforms drugs to theranostic agents. J Nucl Med. 2016.
60. Chatalic KL, Heskamp S, Konijnenberg M, Molkenboer-Kuenen JD, Franssen GM, Clahsen-van Groningen MC, et al. Towards Personalized Treatment of Prostate Cancer: PSMA I&T, a Promising Prostate-Specific Membrane Antigen-Targeted Theranostic Agent. Theranostics. 2016; 6: 849-61.
61. Maeda H, Nakamura H, Fang J. The EPR effect for macromolecular drug delivery to solid tumors: Improvement of tumor uptake, lowering of systemic toxicity, and distinct tumor imaging in vivo. Adv Drug Deliv Rev. 2013; 65: 71-9.
62. Kratz F. A clinical update of using albumin as a drug vehicle - a commentary. J Control Release. 2014; 190: 331-6.
63. Kiess AP, Minn I, Vaidyanathan G, Hobbs RF, Josefsson A, Shen C, et al. (2S)-2-(3-(1-Carboxy-5-(4-211At-Astatobenzamido)Pentyl)Ureido)-Pentanedioic Acid for PSMA-Targeted alpha-Particle Radiopharmaceutical Therapy. J Nucl Med. 2016; 57: 1569-75.
64. Dennis MS, Jin H, Dugger D, Yang R, McFarland L, Ogasawara A, et al. Imaging tumors with an albumin-binding Fab, a novel tumor-targeting agent. Cancer Res. 2007; 67: 254-61.
65. Kratochwil C, Giesel FL, Leotta K, Eder M, Hoppe-Tich T, Youssoufian H, et al. PMPA for nephroprotection in PSMA-targeted radionuclide therapy of prostate cancer. J Nucl Med. 2015; 56: 293-8.
66. Aggarwal S, Ricklis RM, Williams SA, Denmeade SR. Comparative study of PSMA expression in the prostate of mouse, dog, monkey, and human. Prostate. 2006; 66: 903-10.
67. Gregor PD, Wolchok JD, Turaga V, Latouche JB, Sadelain M, Bacich D, et al. Induction of autoantibodies to syngeneic prostate-specific membrane antigen by xenogeneic vaccination. Int J Cancer. 2005; 116: 415-21.
68. Troyer JK, Beckett ML, Wright GL, Jr. Detection and characterization of the prostate-specific membrane antigen (PSMA) in tissue extracts and body fluids. Int J Cancer. 1995; 62: 552-8.
69. Israeli RS, Powell CT, Corr JG, Fair WR, Heston WD. Expression of the prostate-specific membrane antigen. Cancer Res. 1994; 54: 1807-11.